Diffusion of Zn into GaAs and AlGaAs from isothermal liquid-phase epitaxy solutions

C. Algora, G. L. Araújo, and A. Martí
Universidad Politécnica de Madrid, Departamento de Electrónica Física, Escuela Técnica Superior de Ingenieros de Telecomunicación, Ciudad Universitaria s/n, 28040 Madrid, Spain

(Received 19 October 1989; accepted for publication 15 May 1990)

In this work we present results of zinc diffusion in GaAs using the liquid phase epitaxy technique from liquid solutions of Ga-As-Zn and Ga-As-Al-Zn. Using silicon-doped *n*-GaAs substrates, working at a diffusion temperature of 850 °C, and introducing a dopant concentration ranging 10^{18}–10^{19} cm^{-3}, the most important findings regarding the diffusion properties are as follows: (a) zinc concentration in the solid depends on the square root of zinc atomic fraction in the liquid; (b) the diffusion is dominated by the interstitial-substitutional process; (c) the diffusivity D varies as about C^3 in the form $D = 2.9\times10^{-67}C^{3.05}$; (d) aluminum plays the role of the catalyst of the diffusion process, if it is introduced in the liquid solution, since it is found that D varies as $(\gamma_{As}X^l_{As})^{-1}$; (e) the zinc interstitial is mainly doubly ionized (Zn_i^{++}); (f) the zinc diffusion coefficient in $Al_{0.85}Ga_{0.15}As$ is about four times greater than in GaAs; (g) by means of all these results, it is possible to control zinc diffusion processes in order to obtain optimized depth junctions and doping levels in semiconductor device fabrication.

I. INTRODUCTION

Diffusion of Zn into GaAs and AlGaAs is an important process in the fabrication of double-heterostructure lasers,[1,2] integrated optical devices,[3] and solar cells[4,5] to form doped layers or *p-n* junctions. A lot of these devices are usually formed on *n*-GaAs substrates by the liquid-phase epitaxial (LPE) method. This is most simply done by allowing the zinc to diffuse into the n-GaAs substrate during growth of the AlGaAs layer to produce the needed *p-n* junction. It is important to control the junction depth, that is, the thickness of the *p*-GaAs diffused region, because the device characteristics depend most strongly on the junction depth. Therefore, it is necessary to know the diffusion coefficient and the diffusion mechanism of zinc in order to control the junction depth for the AlGaAs/GaAs heterojunction devices, even when the *p*- and *n*-type layers are individually grown on the substrate.

The traditional, rather cumbersome approach to diffuse Zn has been to seal the sample and Zn source in an evacuated ampoule. Other methods, such as open-tube diffusion from a deposited zinc oxide film on the substrate[6] and Zn ion implantation and anneal,[7] have been developed as controllable diffusion techniques. Recently, some new methods of open-tube Zn diffusion into AlGaAs and GaAs using a confined chamber in a modified graphite liquid-phase epitaxy boat[8] and with a "leaky-tube" diffusion furnace[9,10] have been presented. However, while the Zn doping by these techniques has been well documented, few investigations have been reported on the diffusion during LPE growth.[11,12] Moreover, the other techniques can be used to obtain relatively high doping densities (10^{19} cm^{-3}) in a controlled manner but this has not been the case for LPE. Due to the high Zn vapor pressure, which leads to Zn losses during heat-up, the control of Zn doping has been a significant problem in liquid-phase epitaxy. On the other hand, the behavior of zinc diffusing into the ternary AlGaAs has not been intensively examined.[13] In fact, the body of knowledge on zinc diffusion into AlGaAs in the literature is relatively scanty and somewhat inconsistent. In a similar manner, the behavior of zinc diffusion on multiheterostructures of GaAs/AlGaAs has not been extensively studied.

In this paper we report on the diffusion of zinc into the *n*-GaAs substrates from LPE solutions containing either Ga-As-Zn or Ga-As-Al-Zn. The Al content in the epitaxial solution was fixed to obtain an Al composition in the solid, z, *p*-$Ga_{1-z}Al_zAs$ of 0.85 throughout this work for the preparation of AlGaAs/GaAs heterostructure solar cells. The data obtained show that zinc diffuses more rapidly from the liquid solutions containing aluminum, and its behavior is examined and modeled analytically. Applying the Boltzmann–Matano analysis and with the aid of secondary-ion mass spectroscopy (SIMS) measurements, we obtain data relating the diffusion of zinc in GaAs at a temperature of 850 °C. From the analysis of these data we conclude that diffusion of zinc in GaAs occurs by the interstitial-substitutional mechanism and that interstitial zinc carries a double positive charge. Finally, a simple but useful example of zinc diffusion into a heterostructure AlGaAs/GaAs is analyzed showing that zinc diffuses about four times more rapidly in $Al_zGa_{1-z}As$ ($z\cong0.85$) than in GaAs.

II. GROWTH

The diffusions were carried out on (100) silicon-doped *n*-GaAs substrates, whose carrier concentration was 2×10^{17} cm^{-3}. The process was a follows: the melts were brought to the desired saturation temperature $T = 850$ °C. Next the melts were cooled up to 840 °C to affect finer saturation control. Then the substrate was brought into contact with the first melt (Ga-As), and at the same time the temperature was increased to 850 °C to produce an *in situ* etch-

 0021-8979/90/182723-08$03.00

back of the substrate, prior to diffusion. This has a beneficial effect on device performance by producing a cleaner substrate-melt interface.[14,15] Finally, the second melt (Ga-As-Zn or Ga-Al-As-Zn depending on the experiment) was positioned over the substrate and held there during some minutes at 850 °C. This causes the diffusion of zinc in the substrate and a *p-n* junction is formed. Zn content in the melt ranged from 5 to 100 mg per gram of Ga.

In order to obtain reproducible conditions, the melt containing zinc, and preferably other melts as well, must be capped to minimize the loss of zinc and the contamination of the other melts. Moreover, in our case we have put an ingot of tungsten over the caps to avoid its movement due to zinc pressure during heat-up. In this manner we have been able to reduce zinc evaporation.

In the case of Zn diffusion from an Al-Ga-As melt, an $Al_zGa_{1-z}As$ layer of some tens of nanometers over the *p* region was observed as has been reported elsewhere.[16] The Al mole fraction in the $Al_zGa_{1-z}As$ layer was determined by electron probe x-ray microanalyzer (EPXMA) measurements. SIMS analysis showed that this layer was graded in composition from pure GaAs at the interface to $Al_zGa_{1-z}As$ with $z \simeq 0.85$ at the surface. In some other cases the temperature was decreased slightly to produce an $Al_zGa_{1-z}As$ layer that on some occasions presented sporadic nucleations. These regions allow us to study its influence over zinc diffusion.

III. RESULTS

Very smooth and planar interfaces were observed for all samples studied (Fig. 1). It can be verified that the diffusion front reproduces the shape of the substrate, as can be seen in Fig. 2, a fact that is very interesting with respect to the use of LPE in the fabrication of advanced structure solar cells.[17]

Hall measurements were performed on square (2×2 mm) samples with metallic contact dots at the corners and the junction depths were obtained from direct observation of cleaved surfaces using a scanning electron microscope (SEM). Hall mobilities and hole concentrations, as determined from these data, are presented in Fig. 3. In Fig. 3(a) the mobility variation versus hole concentration at 27 °C is represented; the best-fit value, $\mu = 5.93\times10^5 p^{-0.202}$, will be used below. The hole concentration as a function of the Zn atomic fraction in the liquid, X^l_{Zn}, is represented in Fig. 3(b). The indicated values of X^l_{Zn} were calculated from the starting weight of all the components put in the melt: in our case a thin solution with a 1.44 cm^2 growth area and 2 g of Ga in the melt as the main component.

As can be seen, an empirical and useful relationship between the room-temperature free-hole concentration in the solid and the Zn atomic fraction in the liquid is obtained. Our experimental points can be well fitted by a straight line on the log-log plot such that

$$p(\text{cm}^{-3}) \simeq 1.28\times10^{19}[X^l_{Zn}]^{0.47}. \quad (1)$$

Such a fit agrees fairly well with the square-root dependence that has been theoretically predicted[18] for dopants, like Zn, that diffuse rapidly, permitting thermodynamic equilibrium to be established between the growth solution and the bulk of the solid. In fact, the experimental data can be made to fit a square-root model without appreciably losing the fit quality. For this case, the best fit is $p = 1.40\times10^{19}(X^l_{Zn})^{1/2}$. The theoretical relationship for an As-saturated Ga solution derived by Jordan[19] is also shown in Fig. 3(b).

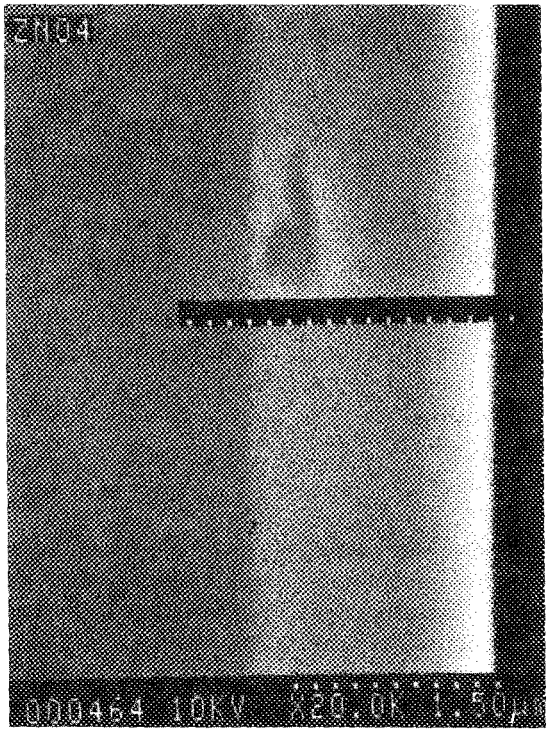

FIG. 1. Microphotography of a zinc-diffused layer (white region)

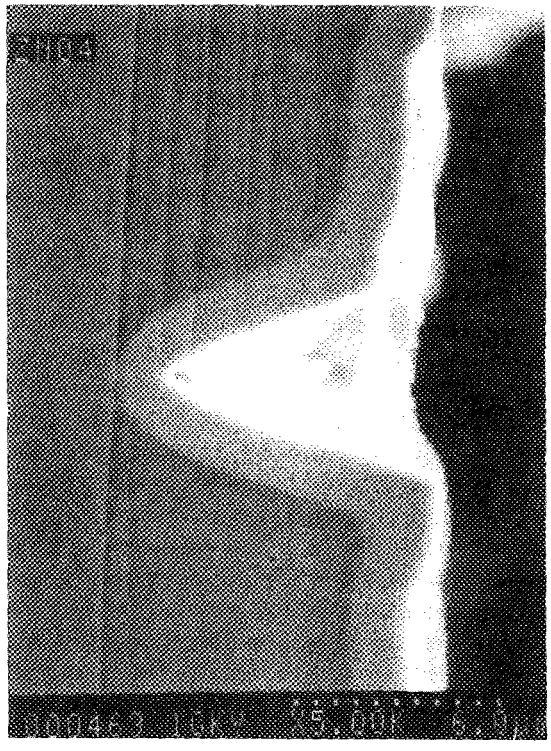

FIG. 2. Microphotography where it can be seen how the front diffusion reproduces the shape of the substrate.

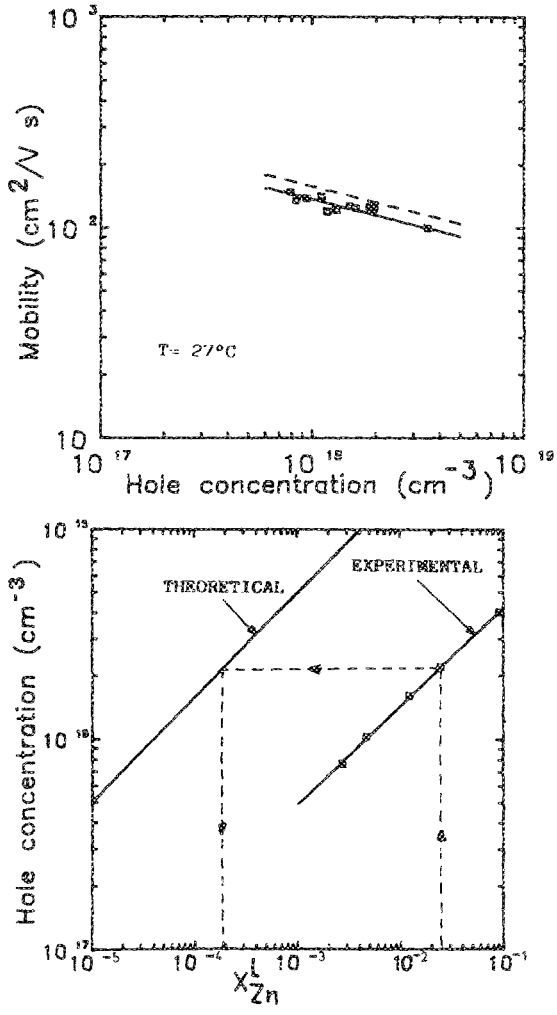

FIG. 3. (a) Measured values of Hall mobility as a function of hole concentration at room temperature. Also included is the mobility (dashed line) obtained by Gardner (Ref. 25). (b) Theoretically predicted (Ref. 19) and experimentally determined hole concentration vs zinc atomic fraction weighed into the As-saturated Ga solution. The dashed line indicates the way to obtain the corresponding zinc atomic fraction that remains in the liquid at the start of diffusion.

As can be observed, there is a large shift between the theoretical curve of Jordan and the experimental curve of this work, indicating that extensive losses of Zn from the melt occur during heat-up.

If the Zn is assumed to be lost to vacuum, the loss rate G (in g cm^{-2} s^{-1}) is proportional to the Zn partial pressure P (in mm), and can be calculated by using the expression[20] $G=(P/17.1)(M_{Zn}/T)^{1/2}$, where M_{Zn} and T are the Zn atomic weight and the absolute temperature, respectively. The Zn partial pressure has been shown to be linearly dependent on the Zn concentration in solution.[19] Therefore, the Zn losses are proportional to the zinc content in the melt, resulting in an experimental curve parallel to the theoretical one over the whole studied range. This fact allows us to evaluate the quantity of zinc that remains in the liquid solution at the diffusion starting moment: if we take the zinc atomic fractions of Fig. 3(b) corresponding to the zinc initially put in the baths (a part of which is lost during heat-up), and the theoretical curve of Jordan is considered as a valid reference, it is possible to obtain the new X^L_{Zn} corresponding to the zinc atomic fraction that remains in the liquid when diffusion starts [see the broken line of Fig. 3(b)]. In this way, our results are directly comparable from now on to those of other researchers.

From the factor-of-100 difference between the theoretical and experimental Zn concentrations, it is possible to calculate an effective evaporation area of about 3×10^{-6} cm^2 for a 4-h heat-up plus diffusion time under our experimental conditions. This effective area is about three times less than that reported elsewhere,[21] showing that our experimental conditions effectively minimize the problems associated with zinc evaporation, allowing to maintain the process under control.

If temperature, time, and substrate concentration are constant, the p-GaAs region thickness depends on zinc atomic fraction. Figure 4 shows this dependence. The junction depth appears to obey a 0.65 power-law dependence on the Zn concentration in the liquid for a diffusion time of 9 min and a 0.67 power law for 64 min.

The partial differential equation of diffusion is

$$\frac{\partial}{\partial x}\left(D\frac{\partial C}{\partial x}\right)=\frac{\partial C}{\partial t}, \tag{2}$$

D being the diffusivity and C the dopant concentration. Denoting by C_{sur} the dopant concentration at the surface and by D_{sur} the Zn diffusivity at the surface, Eq. (2) can be changed into an ordinary differential equation using the Boltzmann transformation[22]

$$y=x/2\sqrt{D_{sur}t}, \tag{3}$$

and a'solution $C(y)$ (C depending only on y) can be found provided D depends only on C, and C_{sur} is time independent during the diffusion process.

As in our case, the bulk concentration C_B (substrate dopage) was always the same, the condition $C(y_j)=C_B$ satisfied at the p-n junction results in a y_j value which is independent of time. As a consequence, Eq. (3) leads to

$$x_j=2\sqrt{D_{sur}}\,y_j\sqrt{t}=\text{const}\ \sqrt{t}. \tag{4}$$

In Fig. 5 the experimental values of x_j vs $\sqrt{t}$ for the

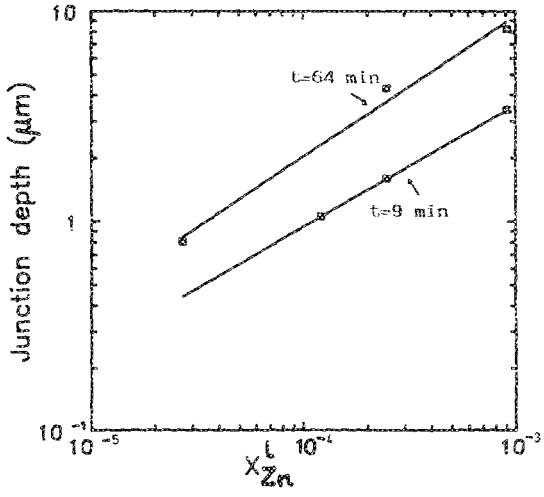

FIG. 4. Junction depth vs zinc atomic fraction in the melt for two different diffusion times.

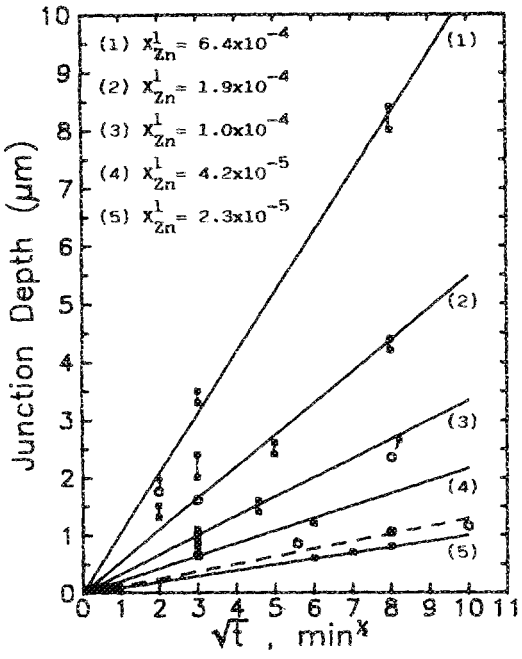

FIG. 5. Measured values of the junction depth as a function of the square root of the diffusion time for different zinc concentrations and at a temperature of 850 °C. The solid lines correspond to diffusions performed from liquid solutions containing aluminum and the dashed line corresponds to diffusions performed from liquid solutions without aluminum and with the same zinc atomic fraction than that of line (4). There are also circles shown representing diffusions from liquid solutions without aluminum, with its corresponding zinc concentrations indicated by arrows.

different zinc concentrations are plotted. As can be seen, the linear relationship theoretically predicted is experimentally found for each zinc concentration. So, we can conclude that the interstitial-substitutional model governs zinc diffusion in GaAs since in this kind of mechanism an equilibrium of vacancies is reached during the diffusion causing D and C_{sur} to be time independent.

Figure 5 also shows the modifications occurring in the diffusion behavior when Al is incorporated into the liquid solution. The effect is clear: Zn diffuses more rapidly from solutions containing Al. This phenomenon will be analyzed below, but it can be explained qualitatively as follows: the liquidus isotherms for the Ga-rich saturated solutions of the Ga-Al-As system show that the atomic percentage of As decreases when Al percentage increases,[23] and consequently the Ga vacancies in the GaAs substrate decrease [see Eq. (22)] when both phases are placed in contact. As the concentration of Ga vacancies decreases, the zinc atoms are not shifted to the substitutional sites and the fast interstitial diffusion is increased. This fact could be used to obtain deeper junctions with the same diffusion time; in this way Al would play the role of a catalyst in the process.

To calculate the relationship between diffusion coefficient and dopant concentration, consider the general situation where the diffusivity can be written directly as some power of the concentration, such as

$$D = D_{sur}(C/C_{sur})^m = D_{sur}\tilde{C}^m(y), \tag{5}$$

where $\tilde{C}(y)$ is the y-dependent normalized concentration. Theoretically, m can reach any value, but in the case of zinc, only some values are permitted due to the fact that m is related to the degree of ionization of the interstitial zinc, r, in the form $m = r + 1$. For zinc the ionization can be single or double, and therefore m can be 2 or 3. The case $m = 0$ corresponds to a constant diffusivity situation but it is widely accepted that diffusivity varies with concentration. So, the only cases that we will study are $m = 2$ and 3. For these values the profiles are very steep and since the bulk concentration C_B is much lower than C_{sur}, the values of y_j corresponding to the junction position are almost independent of C_B and have been obtained by Weisberg and Blanc.[24] These values are $y_j = 0.546$ and 0.436 for $m = 2$ and 3, respectively.

If the value of y_j is known, D_{sur} can be obtained from Eq. (4):

$$D_{sur} = \frac{1}{4y_j^2}\left(\frac{x_j}{\sqrt{t}}\right)^2, \tag{6}$$

where $x_j/\sqrt{t}$ is the slope of the lines plotted in Fig. 5. The values of D_{sur} calculated in this way for the different zinc concentrations and for the liquid solutions containing Al ($z = 0.85$) or not are presented in Table I.

To calculate C_{sur}, the V/I values, as measured by the four-point technique, were used to obtain the average resistivity $\bar{\rho}$ according to the formula

$$\bar{\rho} = K(V/I)x_j, \tag{7}$$

where K is a correction factor that in our case has a value of 4.53. This average resistivity is related to the doping profile. In effect,

$$\frac{1}{\bar{\rho}} = \frac{1}{x_j}\int_0^{x_j}\frac{dx}{\rho}, \tag{8}$$

where the expression for ρ is related to dopant concentration. In this work the expression

TABLE I. D_{sur} (cm^2 s^{-1}) and C_{sur} (cm^{-3}) for different zinc and arsenic concentrations and different values of m.

			$m = 2$		$m = 3$	
X^l_{Zn} (10^{-1})	new X^l_{Zn} (10^{-4})	X^l_{As} (10^{-2})	C_{sur} (10^{18} cm^{-3})	D_{sur} (10^{-10} cm^2/s)	C_{sur} (10^{18} cm^{-3})	D_{sur} (10^{-10} cm^2/s)
0.27	0.23	0.73	1.2	0.014	1.1	0.022
0.46	0.42	0.73	1.6	0.066	1.5	0.010
0.46	0.42	3.8	2.1	0.023	2.6	0.036
1.2	1.0	0.73	2.2	0.16	2.0	0.24
2.5	1.9	0.73	3.2	0.42	2.8	0.66
9.1	6.4	0.73	5.3	1.5	4.8	2.4

$$\rho(\Omega\,cm) = 1.13\times10^{12}C^{-0.744} \tag{9}$$

has been used. In this equation the variation of the mobility with hole concentration was taken into account and the assumption that the impurities are fully ionized is made. The relationship between mobility and concentration has been obtained by computing the best fit to our experimental points but keeping to the slope given by Gardner[25] [Fig. 3(a)]. This slope was considered to be more adequate because the narrow range of concentration of our experimental data would not give enough accuracy for the slope.

From Eqs. (7), (8), and (9) the following expression for C_{sur} is derived:

$$C_{sur} = \left(\frac{1.13\times10^{12}(I/V)/x_j}{(K/y_j)\int_0^{y_j}\tilde{C}(y)dy} \right)^{1/0.744}. \tag{10}$$

According to this equation I/V must be proportional to x_j for diffusion processes performed at the same zinc concentration even at different diffusion times. In Fig. 6 the I/V values versus x_j for different zinc concentrations are represented and a linear dependence between both variables is observed. Therefore, the linear relationship between I/V and x_j expressed in Eq. (10) is confirmed.

To obtain the values of C_{sur} from Eq. (10), we have used the values of the integral for $m = 2$ and 3 calculated in Ref. 26. The values of $(I/V)/x_j$ are derived from the slopes of the straight lines of Fig. 6. The values obtained are summarized in Table I.

To calculate which is the variation law of diffusivity vs. concentration, we have represented D_{sur} vs C_{sur} for $m = 2$ and 3, and we have also calculated their resulting slopes (m_c). The values of m_c allow us to know if the calculation process is consistent with regard to the starting hypothesis (value of m), because in this case $m_c \simeq m$ must occur. The comparison of values shows that only the supposition of $m = 3$ is valid because then $m_c = 3.05$. So, we can conclude that D_{sur} has a dependence close to the cube on C_{sur}. The curve for $m = 3.05$ is represented in Fig. 7 in which the best fitting of the calculated points is $D_{sur} = 2.88\times10^{-67}C_{sur}^{3.05}$.

In this respect, it is important to return to Eq. (5) that substituted in Eq. (4) gives

$$x_j = \text{const}\, C_{sur}^{m/2}\sqrt{t}. \tag{11}$$

Taking into account that

$$p = C_{sur}(D/D_{sur})^{1/m} - C_B \simeq C_{sur}(D/D_{sur})^{1/m}, \tag{12}$$

and introducing Eq. (12) and the theoretical fitting of Eq. (1) in Eq. (11), we obtain

$$x_j = \text{const}\,[X_{Zn}^I]^{m/4}\sqrt{t}, \tag{13}$$

which indicates that slopes of Fig. 4 must be equal to $m/4$. The calculated slopes in this figure were 0.65 and 0.67, which produce $m = 2.6$–2.7. These values, which are closer to 3 than to 2, are in agreement with the almost cubic dependence obtained by the Boltzmann–Matano analysis.

The variation of the junction depth with zinc atomic fraction for diffusions performed by LPE has been also studied by Hovel,[27] who found a slope of 0.59 which produces $m = 2.34$. This fact does not seem to be in agreement with our results, which may be attributed to the fact that those other results were obtained under a higher temperature (900 °C). In Ref. 26 and for diffusions made by the sealed ampoule technique, the exponent m changes from 3 to 2 when the temperature increases. In this way the two results could be in agreement. So, it can be concluded that probably there is a mixture of the two zinc species but at 850 °C the major kind is the doubly ionized interstitial zinc.

As a verification of the results so obtained, SIMS profiles of Zn concentrations were measured. The secondary-ion mass spectrometer was a Cameca 3F. In this study we used a 10-keV O_2^+ beam mass. The beam mass was rastered scanned to cover an area of $250\times250\,\mu m$, but the scaler was gated to count only during the central 5% of the scanned area. Junction depth determined by SIMS agreed extremely well with results of SEM measurements.

By applying the numerical solutions of Weisberg and Blanc to Eq. (5), we fitted the data in Fig. 8 to various theo-

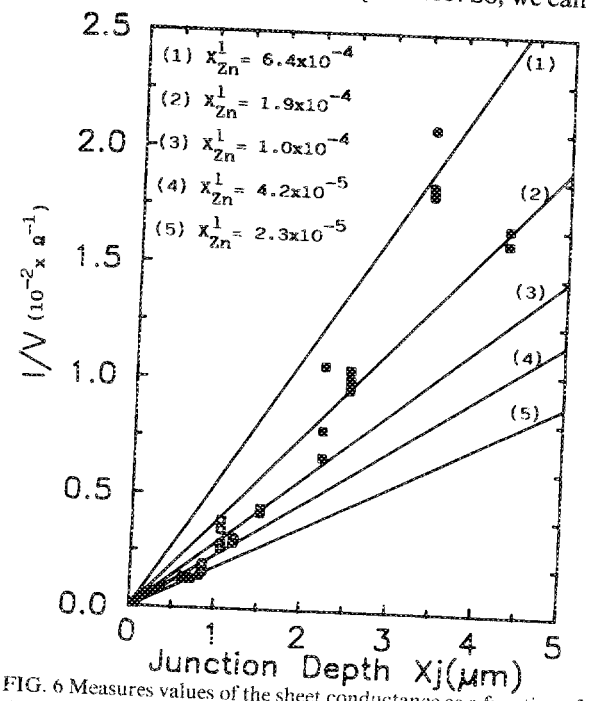

FIG. 6 Measures values of the sheet conductance as a function of the junction depth for different zinc concentrations.

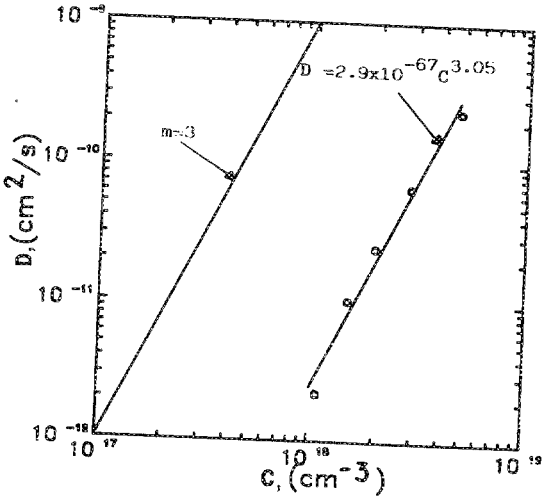

FIG. 7. Effective diffusion coefficient of Zn in GaAs obtained in the present work. A line with a slope equal to 3 is also represented.

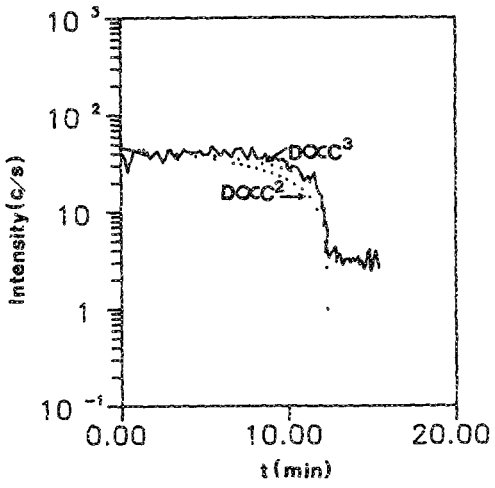

FIG. 8. Concentration profile measured by SIMS of a zinc diffusion in silicon-doped GaAs. Diffusion $T = 850$ °C, diffusion time = 25 min. Substrate carrier concentration = 2×10^{17} cm^{-3}. Theoretical curves for $D \propto C^2$ and $D \propto C^3$ are superimposed. The surface is denoted by the analysis time $t = 0$ min. The zinc concentration is indicated in counts per second.

retical models (different values of m). The parameters used were the surface concentration and surface diffusion coefficient obtained above, and the experimentally measured junction depth. In this way, superimposed on the data of Fig. 8 are theoretical curves for $D_{sur} \propto C_{sur}^2$ (singly ionized interstitial Zn, i.e., $m = 2$) and $D_{sur} \propto C_{sur}^3$ (doubly ionized interstitial Zn, i.e., $m = 3$). Clearly the best fit occurs for $D_{sur} \propto C_{sur}^3$, indicating that the diffusing species are mainly doubly ionized Zn interstitial donors.

A last observation was carried out over some samples that presented sporadic $Al_{0.85}Ga_{0.15}As$ growths over the surface when a small decrease of temperature during the contact was made. The Al content of these segregations was measured by EPXMA. Figure 9 shows a cross section of sample ZN33-4, where the AlGaAs can be recognized as the dark regions close to the surface. Superimposed is the electron-beam-induced current (EBIC) trace that indicates the p-n junction, that is, the limit of the zinc-diffused region. A magnification of Fig. 9 showing the $Al_{0.85}Ga_{0.15}As/GaAs$ heterostructure (Fig. 10) allows us to confirm that zinc diffuses more rapidly through the AlGaAs than through GaAs. This fact has been explained in terms of an increment of interstitial zinc concentration with regard to the substitutional one and, consequently, a higher diffusivity due to the decrease of the number of group-III vacancies at a given temperature when the aluminum composition increases.[28] To evaluate the ratio between zinc diffusivity in $Al_{0.85}Ga_{0.15}As$ and in GaAs, R^2, we have used the two-boundary diffusion model with constant diffusion coefficient developed by Grove[29] and Yoo,[30] who obtained

$$\frac{x_j}{\sqrt{t}} = -\frac{1}{R}\frac{d_1}{\sqrt{t}} + I, \tag{14}$$

where I is a constant and d_1 the thickness of the $Al_{0.85}Ga_{0.15}As$. The experimental results of zinc diffusion through the single heterostructure of Fig. 10 are presented in Fig. 11. These can be shown to follow the straight line expression of Eq. (14), which can be reformulated as

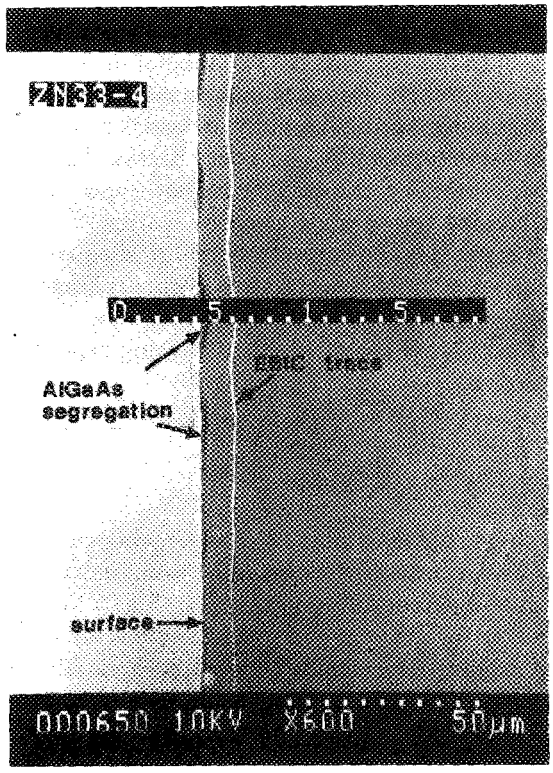

FIG. 9. Cross section of sample ZN33-4 where the EBIC trace that indicates the p-n junction is superimposed. The $Al_{0.85}Ga_{0.15}As$ segregations can be recognized by the dark regions close to the surface.

$$x_j = I\sqrt{t} - Bd_1, \tag{15}$$

where $I = 8.5$ µm h^{-1} and B, the reciprocal or R, has a value of 0.5. This simple model allows us to obtain an estima-

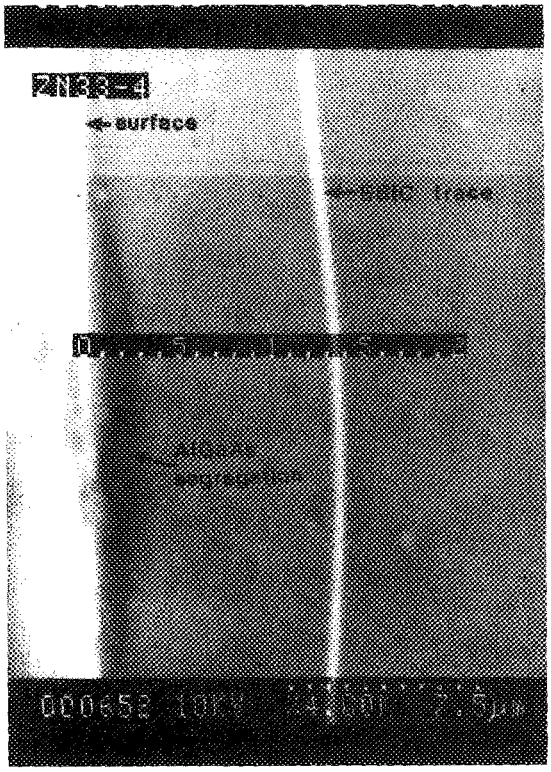

FIG. 10. Microphotography which shows a detail of Fig. 9. It can be seen that diffusion is more rapid when zinc traverses an AlGaAs zone (dark region).

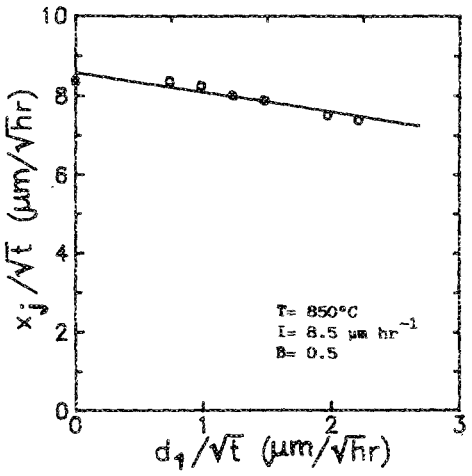

FIG. 11. Penetration of zinc into GaAs covered with an $Al_{0.85}Ga_{0.15}As$ layer at a temperature of 850 °C.

tion of the ratio of zinc diffusivity in the two materials $D_{AlGaAs}/D_{GaAs} \simeq 4$.

IV. DISCUSSION

The most widely accepted model for Zn diffusion in GaAs is the so-called interstitial-substitutional model proposed by Longini[31] in 1962. In this model two forms of Zn impurities are assumed to be present: substitutional zinc and interstitial zinc. The two forms diffuse with different diffusion coefficients D_s and D_i, D_i being much higher than D_s. The diffusion process is therefore limited by the production rate of interstitial zinc, which diffuses very rapidly, although the most abundant kind is substitutional Zn.

In the interstitial-substitutional model, the concentrations of the interstitial and substitutional Zn are related as determined by the equilibrium reaction

$$Zn_s^- + h^+ \rightleftarrows V_{Ga}^0 + Zn_i^{r+} + re^-, \tag{16}$$

where the substitutional Zn, Zn_s^-, is considered as a single acceptor, as it is widely recognized, and where the interstitial Zn, Zn_i^{r+}, can be considered as a single ($r=1$) or a double ($r=2$) donor.

Denoting by k_0 the equilibrium constant of Eq. (16), assuming that all the free holes are supplied by the substitutional ions ($p = [Zn_s^-]$), and taking into account the equilibrium relationship $pn = n_i^2$, it has been demonstrated that the effective diffusion coefficient can be written as

$$D = D_s + D_i \frac{k_0(r+2)}{n_i^{2r}[V_{Ga}^0]}[Zn_s^-]^{r+1}. \tag{17}$$

Unless the $[Zn_s^-]$ is very small, the dominant term in Eq. (17) is the second one. So the process is limited by the diffusion rate of interstitial zinc that decreases with increasing concentration of neutral gallium vacancies, $[V_{Ga}^0]$.

The dependence of D on $[V_{Ga}^0]$ implies its dependence on the atomic fraction of As in the liquid solution, X_{As}^l. In effect, the generation of gallium vacancies is governed by the equation

$$Ga_{Ga} \rightleftarrows Ga(l) + V_{Ga}^0, \tag{18}$$

while the concentration of the species in the liquid is governed by the equilibrium reaction

$$GaAs \rightleftarrows Ga(l) + As(l). \tag{19}$$

The mass-action law relationships for these equations are

$$k_1 = [V_{Ga}^0]a_{Ga}, \tag{20}$$

$$k_2 = a_{Ga}a_{As}, \tag{21}$$

and from these two equations,

$$[V_{Ga}^0] = \frac{k_1}{k_2}a_{As} = \frac{k_1}{k_2}\gamma_{As}X_{As}^l, \tag{22}$$

where a_{Ga} and a_{As} are the chemical activities of gallium and arsenic, respectively, and γ_{As} the activity coefficient of arsenic. Thus the diffusion coefficient of Eq. (17) can now be rewritten, taking Eq. (22) into account, to obtain

$$D = D_s + D_i \frac{k_0 k_2 (r+2)}{k_1 n_i^{2r}\gamma_{As}X_{As}^l}[Zn_s^-]^{r+1}, \tag{23}$$

showing that the As atomic fraction in the liquid in LPE plays a similar role to that played by the arsenic pressure in the sealed ampoule technique.[26]

As can be seen from Fig. 5 and Table I for a constant zinc concentration, diffusions performed from Ga-As-Zn liquid solutions ($X_{As}^l = 0.038$) give diffusion coefficients lower than obtained for Ga-As-Al-Zn liquid solutions ($X_{As}^l = 0.007$). From Eq. (23) the ratio between two different diffusion coefficients must be equal to the ratio between the corresponding arsenic atomic fractions if the rest of the parameters are considered as a constant. However, using Table I for the case of $X_{Zn}^l = 4.2\times10^{-5}$ the ratio between the two different X_{As}^l is about 5 but the ratio between the two diffusivities is about 3. This difference could be explained in terms of experimented variation in γ_{As} when X_{As}^l varies. This variation is not yet well known but the tendency is that γ_{As} increases when X_{As}^l increases.[32] So, in the above example, the γ_{As} variation would help to increase the diffusivity ratio, allowing it to approach to 5. Therefore, variations in diffusion coefficient are jointly due to changes in arsenic atomic fraction in the liquid and in the arsenic activity coefficient.

On the other hand, Eq. (23) shows that D could be proportional to the cube or to the square of zinc concentration depending on whether the zinc is singly or doubly ionized. It is important to note that in the literature the measured concentration variation of D is dependent on the experimental conditions. Most experiments have been carried out by vapor-phase techniques, which gives a dependence on the square of the concentration. Some other research has shown a cube dependence when special diffusion techniques were used. There is no *a priori* justification for the assumption that the zinc atoms carry a double or a single charge. The application of the Boltzmann–Matano analysis to our experiments giving, as the best fit, an almost-cube law and its confirmation by SIMS measurements, provides the best justification for assuming interstitial zinc atoms to be mainly double donors.

V. CONCLUSIONS

We have developed zinc diffusions in GaAs, using the LPE technique, from liquid solutions of Ga-As-Zn and Ga-As-Al-Zn. At a diffusion temperature of 850 °C and with dopant concentration ranging 10^{18}–10^{19} cm^{-3}, the most important findings regarding the diffusion properties are as follows: (a) zinc concentration in the solid depends on the square root of zinc atomic fraction in the liquid; (b) D varies basically on the order of C^3 in the form $D = 2.9 \times 10^{-67} C^{3.05}$; (c) D varies as $(\gamma_{As} X^l_{As})^{-1}$ at a given Al concentration; (d) the diffusion is dominated by the interstitial-substitutional process; (e) the zinc interstitial is mainly doubly ionized (Zn_i^{++}); (f) the zinc diffusion coefficient in AlGaAs ($z = 0.85$) is about four times greater than in GaAs; (g) by means of all these results it is possible to control zinc diffusion processes in order to obtain optimized depth junctions and doping level in semiconductor device fabrication.

ACKNOWLEDGMENTS

This work has been supported by the Spanish Comisión Interministerial de Ciencia y Tecnología (CICYT), Project No. MCl/85. In the early stages of this research partial financial support was obtained from INTA. We thank the Departamento de Ingeniería Electrónica and the Departamento de Tecnología Electrónica of the ETSIT the facilities they have given us for using their installations for Hall measurements and SEM-EBIC analysis, respectively. We are indebted to Marc Gavand and to Christinne Dubois, both from the Laboratoire de Physique de la Matière-Institut National des Sciences Apliquées de Lyon (LPM-INSA), for his careful reading of the manuscript and for her technical support in the SIMS measurements, respectively.

[1] R. T. Lynch, Jr., M. B. Small, and R. Y. Hung, IBM J. Res. Develop. **23**, 585 (1979).
[2] C. S. Hong, J. J. Coleman, P. D. Dapkus, and Y. Z. Liu, Appl. Phys. Lett. **40**, 208 (1982).
[3] J. Wilson, J. F. B. Hawkes, *Optoelectronics: An Introduction* (Prentice-Hall, London, 1983), p. 413.
[4] C. Algora, G. L. Araújo, and A. Martí, Proceedings of the Ninth E.C. Photovoltaic Solar Energy Conference, Freiburg (Kluwer, Dordrecht, 1989), pp. 345–348.
[5] S. Yosida, K. Mitsui, T. Oda, and K. Shirahata, Jpn. J. Appl. Phys. **19**, Suppl. 19-2, 187 (1980).
[6] R. Jett Field and S. K. Ghandi, J. Electrochem. Soc. **129**, 1567 (1982).
[7] M. C. Boisy and D. Dignet, J. Electrochem. Soc. **125**, 1505 (1978).
[8] Y. R. Yuan, K. Eda, G. A. Vawter, and J. L. Merz, J. Appl. Phys. **54**, 6044 (1983).
[9] R. J. Roedel, J. L. Edwards, A. Righter, P. Holm, and H. Erkaya, J. Electrochem Soc. **131**, 1726 (1984).
[10] S. K. Ageno and R. J. Roedel, Appl. Phys. Lett. **47**, 1193 (1985).
[11] A. Chikouche, G. D. E. thesis, Toulouse University, France (1984).
[12] K. Masu, M. Konagai, and K. Takahashi, J. Appl. Phys. **54**, 1574 (1983).
[13] K. Masu, M. Konagai, and K. Takahashi, J. Appl. Phys. **51**, 1060 (1980).
[14] J. M. Woodall and H. J. Hovel, J. Cryst. Growth **39**, 108 (1977).
[15] J. M. Woodall and H. J. Hovel, Appl. Phys. Lett. **30**, 492 (1977).
[16] M. B. Small, R. Ghez, R. M. Potemski, and J. M. Woodall, Appl. Phys. Lett. **35**, 209 (1979).
[17] G. L. Araújo, A. Martí and R. Atiénzar, Proceedings of the 8th E. C. Photovoltac Solar Energy Conference, Florence, Italy (Kluwer, Dordrecht, 1988), pp. 1492–1496.
[18] K. H. Zschauer and A. Vogel, in *Proceedings of the Third International Symposium on GaAs and Related Compounds* (Institute of Physics and Physical Society, London, 1970), p. 100.
[19] A. S. Jordan, J. Electrochem. Soc. **118**, 781 (1971).
[20] I. R. Levine, *Physical Chemistry* (McGraw-Hill, New York, 1978), p. 301.
[21] M. Ettenberg and C. J. Nuese, J. Appl. Phys. **46**, 3500 (1975).
[22] J. Crank, *The Mathematics of Diffusion* (Oxford University, London, 1970).
[23] M. B. Panish and M. Ilegems, in *Progress in Solid State Chemistry*, Vol. 7 (Pergamon, New York, 1972) pp. 39–83.
[24] L. R. Weisberg and J. Blanc, Phys. Rev. **131**, 1548 (1963).
[25] Cf., M. H. Pilkuhm and H. Rupprecht, Trans. Met. Soc. AIME **230**, 296 (1964)
[26] A. Luque, J. Martín, and G. L. Araújo, J. Electrochem. Soc. **123**, 249 (1976).
[27] H. J. Hovel and J. M. Woodall, J. Electrochem. Soc. **120**, 1246 (1973).
[28] C. P. Lee, S. Margalit, and A. Yariv, Solid-State Electron. **21**, 905 (1978)
[29] A. S. Grove, *Physics and Technology of Semiconductor Devices* (Wiley, New York, 1968), p. 75–77.
[30] H.-J. Yoo and Y.-S. Kwon, J. Electron. Mater. **17**, 337 (1988).
[31] R. L. Longini, Solid-State Electron. **5**, 127 (1962).
[32] A. S. Jordan, Met. Trans. **2**, 1965 (1971).